Wavelength & mm-Wave Flexible Converged Optical Fronthaul With a Low Noise Si-Based Integrated Dual Laser Source

Devika Dass , *Graduate Student Member, IEEE*, Amol Delmade , *Graduate Student Member, IEEE*, Liam Barry , *Senior Member, IEEE*, Chris G. H. Roeloffzen , Douwe Geuzebroek , and Colm Browning , *Member, IEEE*

(Top-Scored Paper)

Abstract—A widely tunable hybrid InP-Si$_3$N$_4$ dual laser module (DLM) with low linewidth and relative intensity noise (RIN) is used to develop a wavelength and frequency flexible optical fronthaul system for high-capacity wireless networks. The wavelength flexible (over C-band) delivery of 5G signals over an analog radio-over-fiber (A-RoF) system, incorporating wireless transmission at 60 GHz is demonstrated. A phase noise (PN) and frequency offset (FO) cancelling receiver is used to overcome phase/frequency noise from the DLM due to thermal fluctuations, and this reduces the received (error vector magnitude) EVM to as low as 5%. Using the same DLM we demonstrate the mm-wave frequency flexible (over sub-V-band) delivery of 5G and WiGig signals over a simplified converged fronthaul link. The experimental results show excellent performance with bit error ratio (BER) values as low as 8.46×10^{-6} and 1.11×10^{-4}, and lowest EVMs of 2.4% and 6.1%, achieved for sub-V-band 5G and WiGig signals, respectively. In addition to highlighting the high flexibility of the DLM, this work also presents an approach to deploy this source in future optical-wireless access networks paving way for beyond 5G and 6G technologies.

Index Terms—6G, A-RoF, C-RAN, frequency offset, 5G, hybrid integration, linewidth, millimeter-wave, SiN, V-band, WiGig.

I. INTRODUCTION

THE recent inclusion of millimeter-wave (mm-wave) frequencies in 5G specifications has paved the way for the widespread commercialization and deployment of mobile communication systems initially utilizing carrier frequencies between 25 GHz and 39 GHz, while the 60 GHz unlicensed frequency band continues to grow in popularity for short-distance wireless systems like Wi-Fi [1]. The 'beyond' 5G and 6G

KPIs of ultra-low latency, ultra-reliability and enhanced capacity (driven by futuristic applications such as autonomous vehicles (AV) and augmented/virtual reality (A/VR)) will be delivered to an ever-increasing number of users/devices by a combination of new components and technologies interconnected through high-speed optical transport networks. The enormous bandwidth demands envisioned for future applications coupled with the continued proliferation of small cell antenna sites, also means that the expansion to higher mm-wave and terahertz (THz) (>100 GHz), frequencies is inevitable as we transition to the next generation of mobile communications [2].

For many years, photonic solutions have been recognized as an effective means to generate electronic carriers at such high frequencies. More recently, research has focused on how these methods may be integrated with existing optical infrastructure (e.g., optical access networks) for mm-wave generation and distribution – a concept known as 'convergence' [3], [4]. Indeed, our previous works have explored how a pair of optical carriers with a mm-wave frequency difference may be distributed over an A-RoF fronthaul link from a central office (CO) consisting of a central unit (CU) and distributed unit (DU) to a remote radio unit (RU) for heterodyne detection; directly producing a mm-wave mobile signal after the photo-detection stage [5], [6]. Although the A-RoF transmission approach introduces stringent linearity, phase noise and frequency offset requirements [5], it holds a distinct advantage over current digital approaches in terms of both spectral efficiency and the potential for network scaling [7].

Increasingly, flexible optical technologies such as tunable lasers, optical switch fabrics and active remote nodes, are being proposed as a means to incorporate high bandwidth and low latency wavelength division multiplexing (WDM) networking in the metropolitan and access network domains [8]–[11]. From the perspective of a converged network operating in such a dynamic environment, the ability to assign pairs of optical carriers flexibly across a wide wavelength range for remote mm-wave carrier generation (through optical heterodyning) would be highly advantageous. A discrete approach to optical heterodyning in conjunction with fronthaul transmission involves the use of two independent tunable lasers whose wavelengths are separated by

Devika Dass, Amol Delmade, Liam Barry, and Colm Browning are with the School of Electronic Engineering, Dublin City University, D09Y074 Dublin, Ireland (e-mail: devika.dass2@mail.dcu.ie; amol.delmade2@mail.dcu.ie; liam.barry@dcu.ie; colm.browning@dcu.ie).

Chris G. H. Roeloffzen and Douwe Geuzebroek are with the LioniX International BV, 7521 AN Enschede, The Netherlands (e-mail: c.g.h.roeloffzen@lionix-int.com; d.h.geuzebroek@lionix-int.com).
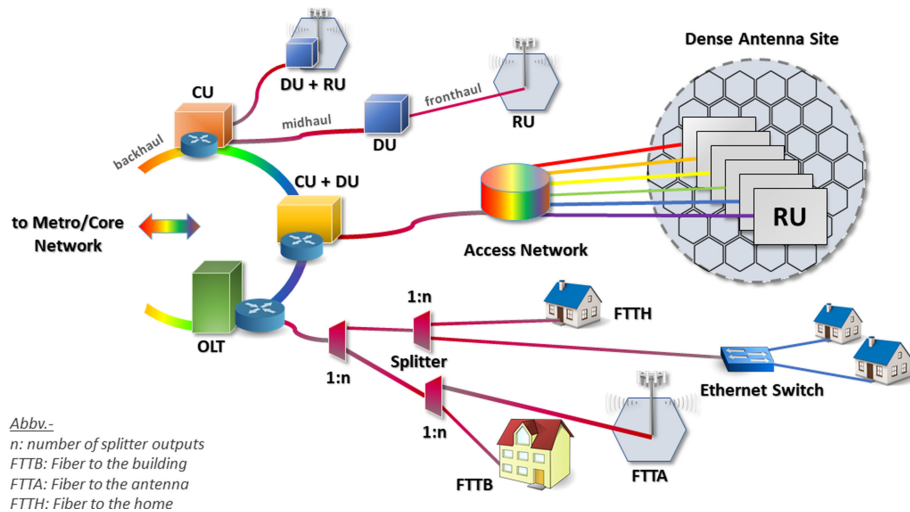
Fig. 1.   A future access network converging the optical and wireless networks is envisioned for beyond 5G and 6G technology.

the desired mm-wave frequency. This method can provide a high level of tunability – but such operation typically requires the use of bulky and expensive sources as well as some form of phase locking to reduce the phase/frequency noise level of the generated mm-wave signal [12]. Comb-based solutions such as gain-switched optical frequency combs (GS-OFCs) [13] and mode-locked lasers (MLLs) [4] can provide pairs of coherent operational wavelength and carrier frequency spacing, respectively. Integrated dual laser solutions providing higher levels of tunability have also been proposed using two distributed Bragg reflector (DBR) lasers [14], [15] with Carpintero *et al.* [13] showing flexible THz operation on a hybrid InP-polymer platform. The advantages of silicon photonics (SiP) are exploited by Hulme *et al.* [16] who demonstrate mm-wave carrier generation from 1–112 GHz with a wavelength tuning range of 42 nm using a dual external cavity laser (ECL) integrated SiP circuit.

In this work, we present the deployment of a tunable InP-Si_3N_4 based hybrid integrated DLM – which offers both ultra-wide wavelength tuning (up to 70 nm for each laser [16]) and relative carrier frequency differences that can be tuned from 10's of GHz to beyond 1 THz [18] – in two heterodyne A-RoF fronthaul link scenarios, incorporating both 10 km fiber and up to 2 m wireless transmission. We elucidate how this source can play a key role in the future optical and wireless integrated CRANs for beyond 5G and 6G applications and services. The two systems are described as follows:

1) In the first scenario, the wavelength flexibility supported by the DLM is exploited in an optical fronthaul transmission system incorporating a phase noise cancelling (PNC) receiver which eradicates the need for a receiver local oscillator (LO) [19]. The resultant system supports wavelength flexible (C-band) 60 GHz A-RoF delivery, with the transmission of 5G new radio (NR) 64-QAM orthogonal frequency division multiplexing (OFDM) exhibiting error vector magnitudes (EVM) as low as 5% over the full link.

2) In the second scenario, the mm-wave frequency flexibility afforded by the DLM, along with PN and FO cancellation, is enabled through the use of an envelope detector at the receiver side of the optical/wireless fronthaul system. The system is shown to support the successful transmission of ~195 MHz bandwidth 5G NR compatible (256-QAM and 512-QAM) and 1.6 GHz IEEE 802.11ad Wi-Fi standard (64-QAM) compatible OFDM signals over a tunable mm-wave frequency range of 55-65 GHz, with EVMs as low as 2.4% recorded.

II. CONVERGENCE OF OPTICAL AND WIRELESS NETWORKS

Photonic convergence with traditional wireless/mobile networks facilitates higher bandwidth, speed of routing and transport, use of pre-existing multi-user access infrastructure, and highly flexible networking, and also is an enabling technology for mm-wave and THz systems. The development of flexible converged optical and wireless networks can be realized by deploying highly flexible network components, that are tunable in the operating wavelength used for optical transmission and radio frequency (RF) used for wireless transmission [20]. A future converged access network, as shown in Fig. 1, will be a coexistence of radio access network (RAN) and optical access network (OAN) supporting various services and applications [21]–[25].

For high-capacity wireless systems with dense antenna deployment and a large number of mobile users/devices, the *centralized* radio access network (C-RAN) architecture - with CU and DU placed at CO and RU at the cell site, as depicted Fig. 1 - provides reduced cost and complexity of RUs at the antenna sites [20], [26], helping to facilitate network scaling. The authors' recent works have demonstrated how this RAN architecture can be deployed in conjunction with centralized, flexible optical heterodyne mm-wave generation and A-RoF transmission; serving to increase system spectral efficiency and flexibility while further reducing RU complexity [5], [6]. These aspects are particularly advantageous for future C-RAN deployments considering the ultra-dense deployment of the antenna sites required for high-frequency wireless systems [7]. To fulfill the high capacity demanded by these dense antenna sites, an
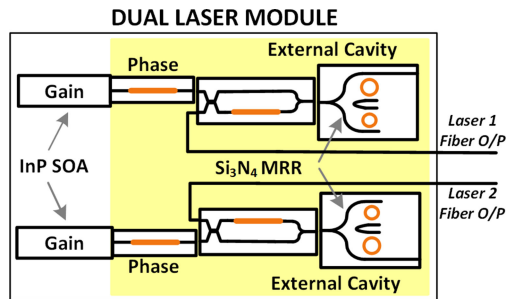
Fig. 2. Simplified schematic of DLM. A detailed schematic of this device is depicted in [17].

TABLE I
LORENTZIAN LINEWIDTH OF DLM

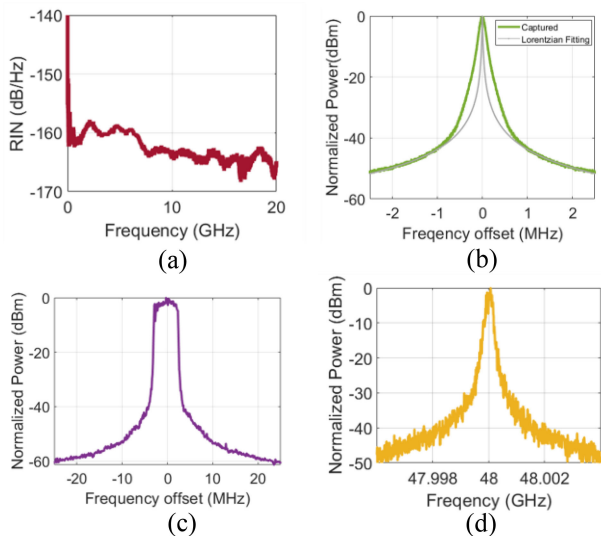| Laser 1		Laser 2	
Wavelength (nm)	Linewidth (kHz)	Wavelength (nm)	Linewidth (kHz)
1492	9	1517	10
1501	14	1527	10
1503	15	1536	14
1512	19	1547	11
1522	18	1557	19
1532	25	1567	20

Fig. 3. Characteristics of the DLM showing (a) RIN of laser 2 at 1552 nm, (b) Optical linewidth of laser 2 at 1536 nm with Lorentzian curve fitting, (c) FO on the 48 GHz beat tone and (d) Electrical spectrum of the 48 GHz beat tone.

active remote node can be deployed to route wavelengths from CO to each RU in a WDM access network environment [27]. This work presents a thorough discussion on the mm-wave A-RoF fronthaul over the C-RAN architecture with a flexible optical source deployed at CO for optical heterodyning.

III. DLM FOR FLEXIBLE OPTICAL/MM-WAVE SYSTEMS

The InP-Si_3N_4 hybrid integrated DLM comprises two on-chip lasers, each with its own output fiber, and is graphically represented in Fig. 2. Each laser consists of an independent InP semiconductor optical amplifier (SOA) which is hybrid coupled to a Si_3N_4 feedback circuit. A detailed device description and characterization is given in our previous work [17] and shows laser tuning ranges of 70 nm each, extremely low RIN of less than -160 dB/Hz (as shown in Fig. 3(a)), typical laser linewidth around 15 kHz (as shown in Fig. 3(b)), and high side mode suppression ratio (SMSR) of > 50 dB. Detailed linewidth measurements have also been carried out on both lasers as the wavelengths are tuned, as this specification will significantly influence the performance of the laser in an A-RoF heterodyne system. From

Table I, a small fluctuation in linewidth (due to different operating conditions for each wavelength) can be observed, but the values remain < 25 kHz for both lasers across the full tuning range.

Since the gain sections (SOAs) of L1 and L2 are independent, the optical carriers emitted are non-coherent, giving rise to phase noise (PN) and frequency offset (FO) on the resultant RF beat-tone after heterodyning of two laser outputs. The FO caused by the relative drift between laser frequencies can be observed by measuring the detected RF beat signal using the max hold function on an electrical spectrum analyzer (ESA). Fig. 3(c) depicts the FO of about 5 MHz on a 48 GHz beat tone and similar FOs are observed as the lasers are tuned to vary the RF beat frequency are expected. Fig. 3(d) presents the RF beat spectrum of two carriers from the dual laser source also with 48 GHz separation. Measuring the 40 dB linewidth of the beat signal to be around 3.4 MHz gives a 3 dB linewidth of ∼34 kHz, as expected for the beat signal of two independent lasers with linewidths of around 15 kHz. To alleviate the PN and FO issues synonymous with the heterodyning of incoherent sources, while still maintaining the tunability afforded by two independent lasers, two receiver types have been used in the systems experiments of this work:

A. PNC Receiver

The PNC receiver (described in detail in [28]) allows the coherent recovery of the received mm-wave signal through the use of a mm-wave pilot tone generated through the heterodyne process at the PD stage. This receiver operation allows optical field modulation to be performed at the CO, helping to improve receiver sensitivity. This comes at the cost of a relatively complex, albeit LO-free, mm-wave receiver architecture and the additional insertion loss associated with optical field modulation at the CO.

B. Envelope Detector

The envelope detector provides a simple and low-cost LO-free mm-wave receiver solution but is well known to suffer from relatively poor sensitivity. The requirement for optical intensity modulation at the CO also limits the achievable optical signal-to-carrier ratio (and hence the optical receiver sensitivity). However, this requirement – which is enabled through simplistic
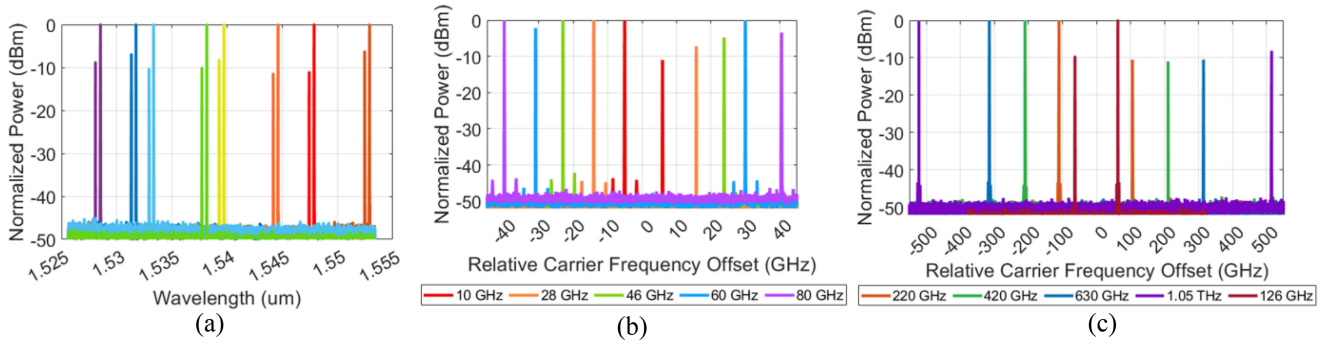
Fig. 4. Thermo-optic tuning of the DLM to generate (a) 56 GHz frequency generation over wavelength, (b) 10 to 90 GHz carrier frequency generation and (c) 100 to 1000 GHz carrier frequency generation.
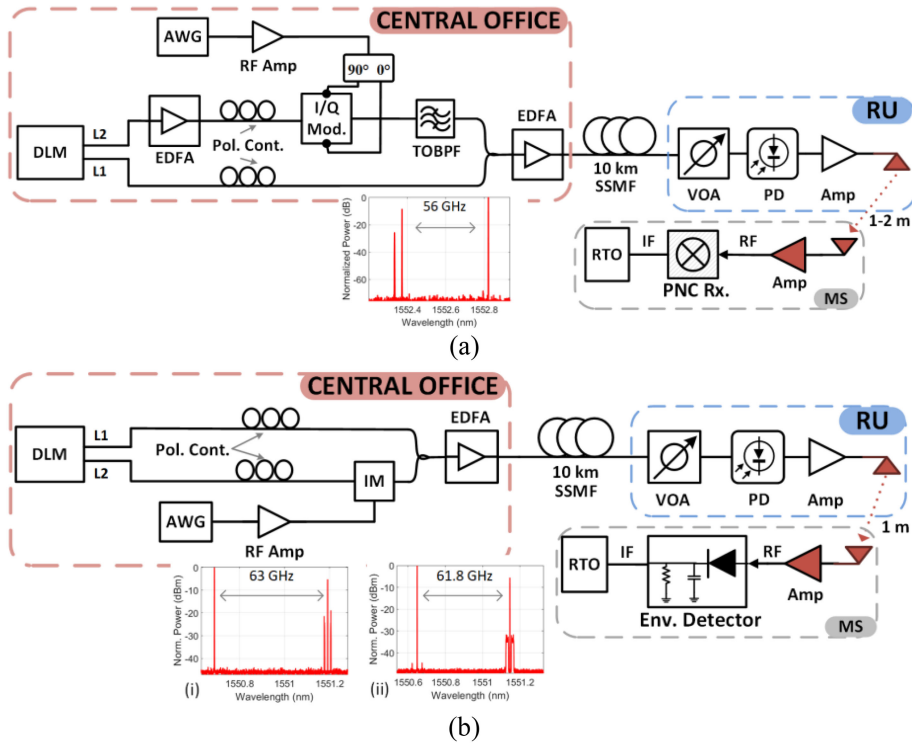

Fig. 5. DLM schematic and two optical/mm-wave experimental A-RoF fronthaul systems, (a) System 1 with I/Q modulator and PNC receiver with inset showing the transmitted optical spectrum and (b) System 2 having IM and envelope detector with inset showing with (i) Narrowband 256-QAM and (ii) Wideband 64-QAM ODSB modulations. Elements in red indicate components added to the system for wireless transmission.

optical modulation, incurring relatively low insertion losses – also serves to lower the complexity of the overall system design.

The flexibility of the DLM, in terms of wavelength tunability and RF signal generation (10 GHz to 1 THz), is depicted in Fig. 4(a), (b) and (c), respectively. This wavelength flexibility of the DLM makes it a superior contender among the other optical sources used for heterodyning discussed in the introduction. In the first fronthaul transmission scenario, fine thermo-optic tuning of each lasers' associated sections was undertaken such that a relative carrier frequency difference of 56 GHz was exhibited at varying central wavelengths within the C-band (Fig. 4(a)). In the second scenario, the DLM is thermo-optically tuned to generate

two optical carriers with the frequency separation ranging from 55 GHz to 65 GHz, covering a part of the V-band.

IV. A-RoF MM-WAVE TRANSMISSION SYSTEMS

To exploit the wavelength and frequency flexibility of the DLM in the converged optical/mm-wave A-RoF fronthaul, the two types of experimental setups were implemented [28], [29].

The first system depicted in Fig. 5(a) employs the I/Q modulator, PNC receiver and other components to evaluate the wavelength flexible performance of DLM over A-RoF fronthaul. In the second system represented in Fig. 5(b), the main differences

TABLE II
INTERMEDIATE FREQUENCY PROPERTIES

Properties	System 1	System 2	
	5G NR	5G NR	WiGig
QAM order	64	256, 512	64
FFT size	2048	2048	512
Total SC [a]	800	800	336
SC Spacing	244 kHz	244 kHz	4.88 MHz
Bandwidth	195 MHz	195 MHz	1.64 GHz
Datarate (Gbps)	1.17	1.56, 1.76 [b]	9.84

[a]SC stands for subcarrier
[b]Values for 256-QAM and 512-QAM respectively.

are the use of the intensity modulator (IM) and the envelope detector-based receiver, and this setup is used to evaluate the frequency flexible performance of the DLM over a simplified A-RoF fronthaul transmission system. For simplicity, we have used system 1 and system 2 to signify the wavelength and frequency flexible optical/mm-wave systems respectively. The PNC receiver is capable of providing superior performance due to higher receiver sensitivity but is bandwidth limited (due to the fixed RF filters used in the circuit) and hence is not used to evaluate the frequency flexibility of the DLM.

A. λ-Flexible Optical/mm-Wave System

In system 1, shown in Fig. 5(a), the DLM is thermo-optically tuned to generate pairs of optical carriers with 56 GHz separation over the C-Band, with optical powers of -3 dBm from laser 1 (L1) and -1 dBm from laser 2 (L2) approximately. L1 is amplified to overcome the losses introduced by the modulation arm of the transmitter. An electrical 5G NR standard compatible 64-QAM OFDM signal (whose parameters are detailed in Table II) was produced by an arbitrary waveform generator (AWG) operating at 20 GSa/s at an intermediate frequency (IF) of 4.75 GHz. The IF is selected such that the modulating OFDM signal far enough from the optical carrier such that signal-to-signal beat interference (SSBI) is avoided, but not too far from the optical carrier such that the received electrical signal is within the passband of the RF components. Depending on system settings used this IF can typically be anywhere in the range of 2-5 GHz. The signal was amplified and used to drive an I/Q Mach-Zehnder Modulator (MZM) biased close to the null point to perform optical single-sideband (O-SSB) modulation on the optical carrier (L1). Complete suppression of the upper sideband was achieved using an optical bandpass filter (OBPF) following modulation - considering the 20 dB modulator extinction. Polarization controllers are placed on both the unmodulated and modulated paths and are manually adjusted to match the polarization of both the paths. However, by deploying a photonic integrated transmitter or polarization-maintaining fiber in this system, manual polarization adjustments can be avoided. The modulated and the unmodulated optical carriers, which are 56 GHz apart, are coupled and amplified by the Erbium-doped fiber amplifier (EDFA) to a total power of +3 dBm before propagation through 10 km of standard single mode fiber (SSMF). The two optical carriers beat together at the 70 GHz PIN photodetector

and produce a mm-wave carrier at 56 GHz and OFDM sideband at 60.75 GHz (56 GHz + 4.75 GHz). The composite mm-wave signal (carrier and data signal) is amplified and then transmitted over a wireless link of 1 - 2 m using a set of 20 dB gain directional horn antennae. The transmission of the mm-wave data signal alongside a PN correlated carrier (pilot tone), enables PN and FO cancellation using the analog electrical PNC receiver structure which is described in detail in [6], [19]. Mixing of the mm-wave carrier and data sideband terms at the PNC stage produces a clean IF OFDM signal which is then captured by a real-time oscilloscope (RTO) at 50 GSa/s before offline processing consisting of synchronization, channel estimation and equalization and EVM/BER measurement is performed.

B. mm-Wave Flexible Optical/mm-Wave System

In system 2, the DLM is thermo-optically tuned to produce the optical carriers with the desired mm-wave frequency carrier separation from 55 GHz to 65 GHz. The inclusion of a single-ended MZM for intensity modulation, coupled with envelope detection, serves to lessen the complexity of the system relative to that of system 1 above. In addition, the intensity modulation operation results in a reduction in modulator insertion losses negating the requirement for the additional EDFA at the transmitter. The single-ended LiNbO$_3$ MZM is fed by two types of IF OFDM signals resembling the 5G NR and Wi-Fi Gigahertz (WiGig) [1] standards. The two IF signals centered at 1.75 GHz, whose properties are given in Table II, are first amplified and then used to drive the MZM which is biased at quadrature for optical double sideband (ODSB) modulation (optical spectra in Fig. 5(b)). An EDFA amplifies the combined optical spectra before its transmission over fiber. The signal is remotely detected by a PD, which photomixes the composite optical signal, generating an mm-wave carrier in the sub-V-band range (55 GHz-65 GHz) with two OFDM signal sidebands 1.75 GHz away from the carrier. The mm-wave generation is limited to this range due to the limited bandwidth of the electrical components at the receiver. This signal is wirelessly transmitted by the antennae over a shorter link length of 1 m, due to lower receiver sensitivity compared to system 1. The received mm-wave signal is fed to a 50-75 GHz envelope detector with 3 GHz IF bandwidth which retrieves the amplitude modulated information to generate an IF OFDM signal. This IF signal is then captured by the RTO for further offline processing.

V. RESULTS AND DISCUSSION

A. λ-Flexible Performance (5G NR)

Initially, the wavelength flexibility of the mm-wave A-RoF system is outlined in Section IV.A. is demonstrated by operating the DLM at four different sets of wavelength pairs across the C-band. Both the lasers from the DML were tuned to achieve a constant relative frequency spacing of 56 GHz while operating at different wavelengths of 1539 nm, 1544 nm, 1548 nm and 1552 nm (shown in Fig. 4(a)). One of the optical carriers from these wavelength pairs were single sideband modulated with a 244 kHz subcarrier spacing OFDM signal (5G NR compatible)
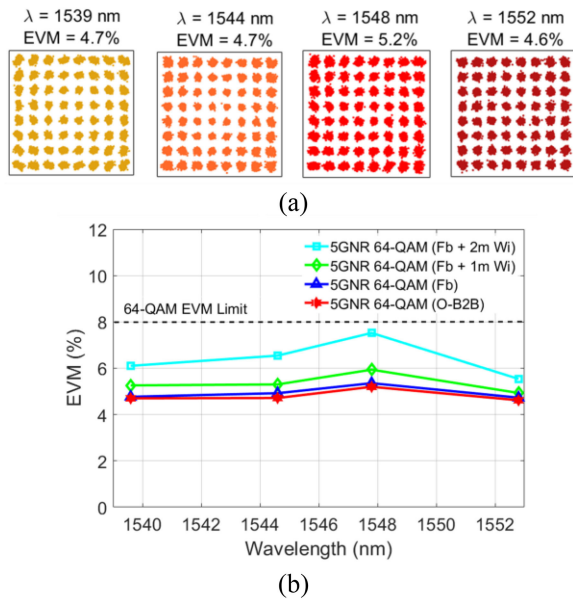
Fig. 6. (a) Constellations of the demodulated 60.75 GHz mm-wave signal and EVM values, (b) EVM performance of the received signal with respect to the wavelength.

at 4.75 GHz intermediate frequency in order to generate a 60.75 GHz mm-wave signal as mentioned in Section IV.A. At first, the performance of the demodulated signal was analyzed in the optical back-to-back (O-B2B) transmission case. The constellation results in Fig. 6(a), representing EVMs between 4.6% and 5.2% at different wavelengths, indicate the successful generation, and demodulation of the 5G NR compatible mm-wave OFDM signal over O-B2B A-RoF fronthaul link. The excellent EVM performance, well within the 8% FEC limit of 64-QAM data, across the C-band highlights the wavelength tuning capabilities of the DML device and outlined system. These results also highlight the ability of the PNC receiver to mitigate the effects of PN and FO which arise from the independent nature of the lasers' on-chip gain sections (as shown by the RF beat tone spectra in Fig. 4(c) and (d)). A small degradation in the performance at the 1547.8 nm wavelength pair is attributed to a reduction in the combined EDFA gain response at that wavelength, as evidenced by the corresponding normalized spectrum (red) in Fig. 4(a). Consequently, a slightly elevated EVM value is obtained for all transmission results obtained at this wavelength (see Fig. 6(b)).

Fig. 6(b) shows the EVM performance of this outlined system (system 1) for four different transmission scenarios of O-B2B, 10 km fiber (Fb), 10 km fiber + 1 m wireless (Fb + 1m Wi), and 10 km fiber + 2 m wireless (Fb + 2m Wi) using all the above-mentioned wavelength pairs. The results indicate that the transmission over 10 km of fiber has a negligible effect on system performance compared to the O-B2B case for all four-wavelength pairs at a received optical power (ROP) of -2 dBm. For wireless transmission, the two horn antennae (each with a passband of 55 GHz-65 GHz) along with an additional receiver electrical booster amplifier were added to the system. The line-of-sight wireless link was manually adjusted to maximize the received power for transmission distances of 1 m and

2 m. Fig. 6(b) shows that the addition of a 1 m wireless link following 10 km fronthaul transmission (Fb + 1m Wi, green curve) results in a small (~0.5%) degradation in EVM across all tested wavelength pairs. This degradation can be attributed to the reduced electrical signal-to-noise ratio (SNR) at the receiver due to additional noise from the booster amplifier. Nevertheless, excellent performance below 6% was achieved in all cases over the full fiber-wireless link.

Increasing the wireless distance to 2 m (Fb + 2m Wi, cyan curve) results in a further 1–1.5% degradation in EVM across the wavelength range. This degradation can be attributed to the combined effects of marginally elevated PD nonlinearity (as the ROP, in this case, was increased to 0.5 dBm to obtain a reasonable signal level at the PNC receiver), as well as additional signal attenuation over the increased wireless link distance. Again, EVM performance between 6% and 7.8%, which is below the 8% EVM limit for 64-QAM, indicates the successful transmission of 1.17 Gb/s 5G NR compatible subcarrier spacing OFDM signals. It should be noted that a more advanced wireless mm-wave link design, such as beam-forming operation using a phased array antenna (PAA), could greatly increase the achievable wireless transmission distance for the presented system [30]. Moreover, incorporating high power RF amplifiers and antennae, photodetectors with higher power handling capabilities and impedance matching between the photodetector and the antennae can increase the radiation power of the antennae, aiding longer distance wireless transmission [31].

This demonstrated wavelength flexibility afforded by the DLM can play an important role in the converged optical access network, where multiple services are transported through the same fiber infrastructure. The excellent performance at four different wavelength pairs across C-band demonstrates the extreme source flexibility which can be provided for network providers seeking to incorporate centralized heterodyne operation for future mm-wave enabled C-RANs. Additionally, in this work, the choice of wavelength tuning over the C-band was dictated by EDFA's gain spectrum, but practically any wavelength pair with desired spacing within the overlapped spectrum of the two lasers could be used.

B. mm-Wave Flexible Performance (5G NR)

While the wavelength flexibility demonstrated by tuning the DLM to operate at four different optical carrier pairs over C-band plays an important role from an optical network design perspective, the mm-wave carrier frequency flexibility is important for an efficient design of the wireless link. In this subsection, we demonstrate variable frequency mm-wave signal generation in the 58.3 GHz to 64.3 GHz sub-V band, over an A-RoF fronthaul system incorporating the envelope detector-based receiver, as described in Section IV.B.

Initially, we tuned both lasers from the integrated DLM to achieve a frequency spacing of 61.8 GHz at 1552 nm. A 244 kHz subcarrier spacing (5G NR compatible) 195 MHz bandwidth OFDM signal at an IF of 1.75 GHz was intensity-modulated on one of the optical carriers and then combined with the other optical carrier to generate a mm-wave signal as mentioned in
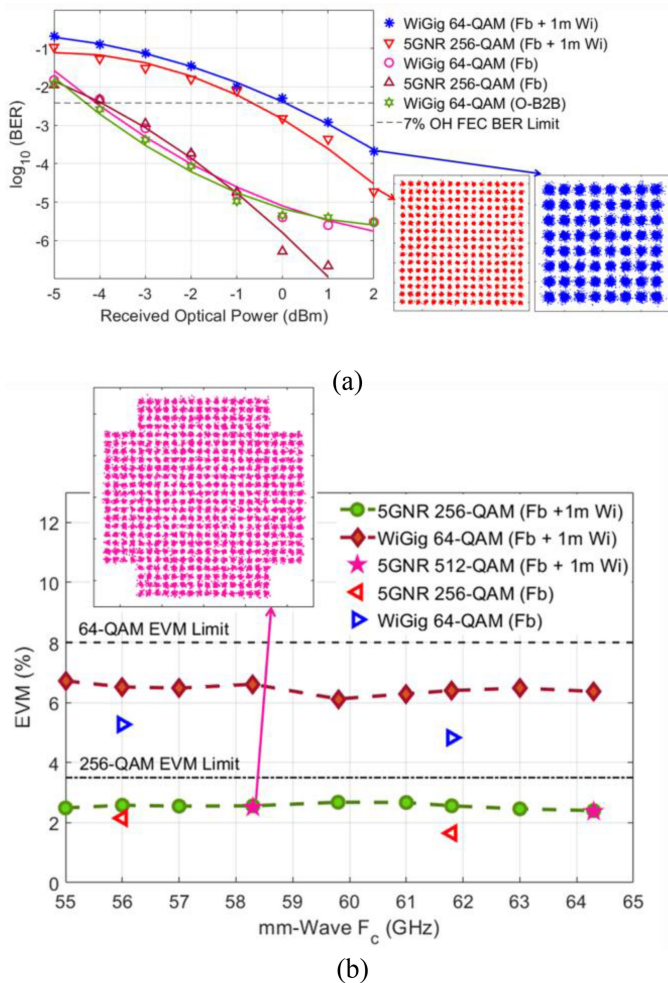
(a)

(b)

Fig. 7. (a) BER versus ROP at 61.8 GHz over both fiber and wireless, only fiber and back-to-back links. The right insets show the constellation of demodulated 61.8 GHz mm-Wave 64-QAM WiGig (blue) and 256-QAM 5G NR (red) signals, respectively, at +2 dBm ROP and (b) EVM as a function of mm-Wave Fc is set at 2 dBm ROP. The insets show an example received constellation for the 512-QAM 5G signal at 58.3 GHz.

the description of system 2 in Section IV.B. Fig. 7(a) shows the BER performance after demodulation of the 256-QAM 61.8 GHz OFDM signal at 61.8 GHz with respect to received optical power on the PD for two different transmission scenarios: 10 km fiber (Fb) and 10 km fiber + 1m wireless (Fb + 1m Wi).

The results show excellent performance in the case of 10 km fiber transmission with BER as low as 8.46×10^{-6} for 1 dBm optical power falling on the PD. As expected, the BER degrades with reduced ROP and reaches the 7% overhead (OH) FEC limit of 2.3×10^{-3} at -4 dBm. The results are shown in Fig. 7(a) further indicate performance degradation with ~3 dB penalty in receiver sensitivity once the wireless transmission is introduced in the link (Fb + 1m Wi case). This performance difference is attributed to the combined effect of SNR degradation due to additional noise from the booster amplifier and reduced electrical power on the receiver envelope detector. Nevertheless, performance below the FEC limit is achieved over the full link demonstrating the successful mobile signal transmission at a data rate of 1.56 Gb/s. A received constellation of the

demodulated 256-QAM data is also shown in Fig. 7(a) for the case of Fb + 1m Wi transmission with a ROP of 2 dBm.

In order to demonstrate the variable frequency mm-wave signal generation, both the lasers from DLM were finely tuned to obtain nine different carrier spacings from 55 GHz to 64.3 GHz. Fig. 7(b) shows the EVM performance of 256-QAM data modulated 5G NR OFDM signals at each of the generated mm-wave frequencies after transmission over 10 km fiber and 1m wireless (Fb + 1m Wi) using the A-RoF system 2 described in Section IV.B. The system shows a uniform performance (below the 3.5% EVM limit for a 256-QAM signal) across the frequency span, with the lowest EVM of 2.4% observed at the carrier frequency of 64.3 GHz (with BER of 8.46×10^{-6}). The slight improvement in system performances, compared to those presented in Section V.A over system 1, stems from the improved OSNR as the second EDFA was not required with this system configuration. In order to further increase the data rate, 512-QAM data was modulation on the OFDM subcarriers, and its performance is shown at two different mm-wave frequencies in Fig. 7(b). In this case with Fb + 1m Wi transmission, EVM values of 2.5% and 2.4% were measured at 58.3 GHz (constellation in Fig. 7(b) inset) and 64.3 GHz frequencies, respectively, delivering the data at the rate of 1.76 Gb/s.

RF/mm-wave carrier frequency flexibility is paramount for the wireless system due to closely spaced channels. The results presented in this subsection show the capabilities of the employed DLM to generate mm-wave signals in the sub-V band with ~1 GHz level of tuning by changing the wavelengths. The choice of operating our system in the 55 GHz to 64.3 GHz frequency band was dictated by the availability of various RF, mm-wave and optoelectronic components. In practice, any frequency up to 1.05 THz can be generated with the employed DML as shown by the tuning spectrum in Fig. 4(b).

C. mm-Wave Flexible Performance (WiGig)

The results presented in the previous two subsections show the successful transmission of 195 MHz bandwidth 5G NR compatible OFDM signals designed for mobile applications. In order to achieve higher data rates, up to 10 Gb/s for 5G and beyond 5G services, wider bandwidth signals need to be transmitted over the mm-wave wireless system. While there is no standard defined for higher channel bandwidth mobile telephony applications yet, the 60 GHz wireless gigabit standard (Wigig IEEE802.11ad [1]) gives some indication of the possible future specifications. The IEEE802.11ad standard for indoor broadband services specifies the use of four 2.16 GHz bandwidth channels (~1.83 GHz signal bandwidth) for data transmission in the unlicensed frequency band between 57 GHz to 66 GHz. The availability of this frequency band in many countries has promoted its use in providing high-speed broadband services in indoor short-range settings. In order to demonstrate a higher data rate system, we transmitted WiGig standard compatible bandwidth OFDM signals over the envelope detector-based mm-wave A-RoF system 2 presented in Section IV.B.

The BER performance of the 61.8 GHz 1.64 GHz bandwidth WiGig signal with variable ROP is shown in Fig. 7(a) for three transmission scenarios of O-B2B, Fb, and Fb + 1m Wi. The

results indicate that the transmission over 10 km fiber does not have any significant effect on the performance of the signal compared to the O-B2B case. In both of these cases, the BER degrades to above the FEC limit at a ROP of -4 dBm – similar to the 5G NR transmission case. At higher ROPs in the Fb transmission scenarios, an error floor emerges in the case of the WiGig signal at 61.8 GHz but is not evident for the 5G NR signal. This effect can be attributed to the impact of the wider signal bandwidth. The results in further performance degradation, with a 4 dB penalty in receiver sensitivity, where wireless transmission is introduced in the link. As mentioned in the previous subsection V.B, this performance difference is attributed to the resultant SNR degradation. The 1 dB receiver sensitivity penalty between WiGig and 5G NR transmission for Fb + 1m Wi case, as seen in Fig. 7(a), can be attributed to the different SNR requirements for the QAM formats used, as well as the differing signal bandwidths.

Here again, we used fine wavelength tunability of the DLM, presented in Section 2, to demonstrate the flexibility of the presented system to successfully generate mm-wave signals within the channel frequencies mentioned in the WiGig standard. Fig. 7(b) shows the EVM performance of the outlined Wi + Fb transmission system with respect to the variable mm-wave carrier frequency from 55 GHz to 64.3 GHz for a ROP of +2 dBm – similar to the 5G NR case. The results indicate minimal variation in the EVM (between 6.1% to 6.7%) for different mm-wave channel frequencies. These results demonstrate the successful transmission of the 9.84 Gb/s signals in all transmission cases, once again highlighting the ability of the system to support centralized and flexible provisioning of future mm-wave services.

The use of a low linewidth and photonic integrated laser module along with FO agnostic receivers in the system has minimal impact on the performance of the WiGig compatible multicarrier OFDM signals. But, in general, the single carrier approach (available as a waveform option for WiGig services [1]) can lessen the requirements for precise FO and PN cancellation at the receiver [4] at the cost of reduced spectral efficiency.

VI. Conclusion

The experimental results presented in this work demonstrate the ability of a hybrid integrated InP-Si$_3$N$_4$ dual tunable laser module to provide flexible wavelength and RF carrier assignment, for remote mm-wave generation through heterodyne detection. Wavelength flexibility permits the best use of available fiber in a reconfigurable network environment while the ability to vary the RF carrier frequencies can allow different RF standards to be used, also enabling future network upgrades to higher carrier frequencies in the THz range. In this work, we initially demonstrated the performance of the integrated dual laser source in a heterodyne A-RoF system with an analog PNC receiver circuit. Excellent performances of ∼5% EVM are achieved on all test wavelengths over the full fiber fronthaul link and a 1 m wireless distance, with negligible degradation compared to the back-to-back cases. The results demonstrate how an integrated dual MRR-based laser module can provide a highly re-configurable silicon-based platform for the successful delivery of 5G A-RoF mm-wave services – in this case

delivering a raw mobile data rate of 1.17 Gb/s at 60.75 GHz. A further simplified and cost-effective system is developed using an envelope detector-based receiver. The system performs exceptionally well, with all recorded EVMs below 3% and 7% for the transmission of 256-QAM 5G NR and 64-QAM WiGig signals, respectively, and exhibits excellent uniformity in EVM performance with both signals exhibiting a variance of less than 1% across the frequency range. Although the double sideband nature of the signal transmission here limits achievable spectral efficiency, the results show that this can be somewhat offset by the successful transmission of OFDM signals with higher-order QAM, up to 512 levels. While the RF tunability demonstrated in this work is over a portion of the V-band, the use of higher speed photodiodes [32] and electrical components [33], in conjunction with the integrated dual laser source presented here, can facilitate A-RoF systems operating in the 100 GHz to 1 THz range.

Compared to InP-based solutions, the integrated silicon photonic approach provides the potential for smaller form-factor, greater cost efficiency and a higher yield device fabrication, as well as ease of integration with surrounding optical and electronic components; ultimately paving the way for a fully integrated optical/mm-wave transceiver. Overall, the work shows that wide tunability, both in wavelength and RF signal generation through optical heterodyning, afforded by the integrated DLM in combination with advanced system design is a highly promising approach enabling photonic mm-wave networking over an optical access infrastructure. This holds particular relevance for future converged optical/radio networks exploiting flexibility in the wavelength and RF domains.

References

[1] B. Schulz, "802.11ad - WLAN at 60 GHz a technology introduction," White Paper, WLAN 802.11ad – 1MA220_3e, Nov. 2017.

[2] H. Tataria, M. Shafi, A. F. Molisch, M. Dohler, H. Sjöland, and F. Tufvesson, "6G Wireless systems: Vision, requirements, challenges, insights, and opportunities," *Proc. IEEE*, vol. 109, no. 7, pp. 1166–1199, Jul. 2021.

[3] C. Lim and A. Nirmalathas, "Radio-over-fiber technology: Present and future," *J. Lightw. Technol.*, vol. 39, pp. 881–888, 2021.

[4] P. T. Dat, A. Kanno, N. Yamamoto, and T. Kawanishi, "Seamless convergence of fiber and wireless systems for 5G and beyond networks," *J. Lightw. Technol.*, vol. 37, no. 2, pp. 592–605, Jan. 2019.

[5] A. Delmade et al., "Optical heterodyne analog radio-over-fiber link for millimeter-wave wireless systems," *J. Lightw. Technol.*, vol. 39, no. 2, pp. 465–474, Jan. 2021.

[6] D. Dass, S. O'Duill, A. Delmade, and C. Browning, "Analysis of phase noise in a hybrid photonic/millimetre-wave system for single and multi-carrier radio applications," *Appl. Sci.*, vol. 10, no. 17, Jan. 2020, Art. no. 17.

[7] S. Noor, P. Assimakopoulos, and N. J. Gomes, "A flexible subcarrier multiplexing system with analog transport and digital processing for 5G (and beyond) fronthaul," *J. Lightw. Technol.*, vol. 37, no. 14, pp. 3689–3700, Jul. 2019.

[8] J. (S.) Zou, S. A. Sasu, M. Lawin, A. Dochhan, J.-P. Elbers, and M. Eiselt, "Advanced optical access technologies for next-generation (5G) mobile networks," *J. Opt. Commun. Netw.*, vol. 12, pp. D86–D98, 2020.

[9] P. Iovanna et al., "Future proof optical network infrastructure for 5G transport," *IEEE/OSA J. Opt. Commun. Netw.*, vol. 8, no. 12, pp. B80–B92, Dec. 2016.

[10] C. Browning et al., "A silicon photonic switching platform for flexible converged centralized-radio access networking," *J. Lightw. Technol.*, vol. 38, pp. 5386–5392, 2020.

[11] X. Guan, R. Dubé-Demers, W. Shi, and L. A. Rusch, "Heterogeneous optical access networks: Enabling low-latency 5G services with a silicon photonic smart edge," *J. Lightw. Technol.*, vol. 39, no. 8, pp. 2348–2357, Apr. 2021.

[12] L. Johansson and A. Seeds, "Generation and transmission of millimeter-wave data-modulated optical signals using an optical injection phase-lock loop," *J. Lightw. Technol.*, vol. 21, no. 2, p. 511, 2003.

[13] C. Browning *et al.*, "Gain-switched optical frequency combs for future mobile radio-over-fiber millimeter-wave systems," *J. Lightw. Technol.*, vol. 36, no. 19, pp. 4602–4610, Oct. 2018,.

[14] G. Carpintero *et al.*, "Wireless data transmission at terahertz carrier waves generated from a hybrid InP-polymer dual tunable DBR laser photonic integrated circuit," *Sci. Rep.*, vol. 8, 2018, Art. no. 3018.

[15] Y. Liu *et al.*, "Dual-wavelength DBR laser integrated with high-speed EAM for THz communications," *Opt. Exp.*, vol. 28, no. 7, pp. 10542–10551, Mar. 2020.

[16] J. Hulme *et al.*, "Fully integrated microwave frequency synthesizer on heterogeneous silicon-III/V," *Opt. Exp.*, vol. 25, pp. 2422–2431, 2017.

[17] D. Dass *et al.*, "28 GBd PAM-8 transmission over a 100 nm range using an InP-Si$_3$N$_4$ based integrated dual tunable laser module," *Opt. Exp.*, vol. 29, pp. 16563–16571, 2021.

[18] R. Guzmán *et al.*, "Widely tunable RF signal generation using an inp/Si$_3$N$_4$ hybrid integrated dual-wavelength optical heterodyne source," *J. Lightw. Technol.*, vol. 39, no. 24, pp. 7664–7671, Dec. 2021, doi: 10.1109/JLT.2021.3078508.

[19] C. Browning, A. Delmade, Y. Lin, J. Poette, H. H. Elwan, and L. P. Barry, "Phase noise robust optical heterodyne system for reduced complexity millimeter-wave analog radio-over-fiber," in *Proc. 45th Eur. Conf. Opt. Commun.*, 2019, pp. 1–4.

[20] C. Browning and D. Dass, "Flexible converged photonic and radio systems: A pathway toward next generation wireless connectivity," in *Proc. Photonic Netw. Devices*, 2021, Paper NeM4B.2.

[21] P. Sehier *et al.*, "Transport evolution for the RAN of the future," *J. Opt. Commun. Netw.*, vol. 11, no. 4, pp. B97–B108, 2019.

[22] G.-K. Chang, M. Xu, and F. Lu, "Optical networking for 5G and fiber-wireless convergence," in *Springer Handbook of Optical Networks*: Cham, Switzerland: Springer, 2020, pp. 1031–1056.

[23] M. Erkılınç *et al.*, "Bidirectional wavelength-division multiplexing transmission over installed fibre using a simplified optical coherent access transceiver," *Nature Commun.*, vol. 8, no. 1, pp. 1–10, 2017.

[24] T. Horvath, P. Munster, V. Oujezsky, and N.-H. Bao, "Passive optical networks progress: A tutorial," *Electronics*, vol. 9, no. 7, 2020, Art. no. 1081.

[25] K. Asaka and J.- Kani, "Standardization trends for next-generation passive optical network stage 2 (NG-PON2)," *NTT Tech. Rev.*, vol. 13, no. 3, pp. 80–84, 2015.

[26] F. Saliou *et al.*, "Optical access network interfaces for 5G and beyond," *J. Opt. Commun. Netw.*, vol. 13, no. 8, pp. D32–D42, 2021.

[27] X. Pang *et al.*, "Centralized optical-frequency-comb-based RF carrier generator for DWDM fiber-wireless access systems," *J. Opt. Commun. Netw.*, vol. 6, no. 1, pp. 1–7, 2014.

[28] D. Dass, A. Delmade, L. Barry, C. G. Roeloffzen, D. Geuzebroek, and C. Browning, "Flexible optical and millimeter-wave analog-RoF transmission with a silicon-based integrated dual laser module," in *Proc. IEEEEur. Conf. Opt. Commun.*, 2021 pp. 1–4.

[29] D. Dass, A. Delmade, L. Barry, C. G. Roeloffzen, D. Geuzebroek, and C. Browning, " Flexible V-band mmwave analog-RoF transmission of 5G and WiGig signals using an InP-SiN integrated laser module," in *Proc. Int. Topical Meeting Microw. Photon.*, 2021, pp. 1–4.

[30] I. F. Akyildiz, C. Han, and S. Nie, "Combating the distance problem in the millimeter wave and terahertz frequency bands," *IEEE Commun. Mag.*, vol. 56, no. 6, pp. 102–108, Jun. 2018.

[31] K. Sun and A. Beling, "High-speed photodetectors for microwave photonics," *Appl. Sci.*, vol. 9, no. 4, Feb. 2019, Art. no. 623, doi: 10.3390/app9040623.

[32] S. M. Koepfli *et al.*, "High-speed graphene photodetection: 300 GHz is not the limit," in *Proc. IEEE Conf. Lasers Electro-Opt. Europe Eur. Quantum Electron. Conf.*, 2021, pp. 1–1.

[33] H. Hamada *et al.*, "Millimeter-wave InP device technologies for ultra-high speed wireless communications toward beyond 5G," in *Proc. IEEE Int. Electron Devices Meeting (IEDM)*, 2019, pp. 9.2.1–9.2.4.